



Analysis of W-type waveguide for Nd-doped fiber laser operating near 940 nm

Seongwoo Yoo ^{a,*}, Daniel B.S. Soh ^b, J. Kim ^a, Y. Jung ^a, J. Nilsson ^b,
J.K. Sahu ^b, Jhang W. Lee ^a, K. Oh ^a

^a Department of Information and Communications, Gwangju Institute of Science and Technology (GIST), 1 Oryong-dong, Buk-gu, Gwangju 500-712, South Korea

^b Optoelectronics Research Centre, University of Southampton, Southampton SO17 1BJ, England

Received 2 July 2004; accepted 9 November 2004

Abstract

We propose a three-layered W-type structure for laser fiber to facilitate the three-level radiative transition near 940 nm region of Nd ion, while suppressing the competing four-level transition near 1060 nm by introducing a novel highly wavelength selective loss mechanism. In order to achieve a net gain around 940 nm, requirements in fiber waveguide parameters for the LP₀₁ mode cut-off and bending loss were theoretically investigated. The waveguide designs were experimentally confirmed generating stable CW single mode output power of 705 mW.

© 2004 Elsevier B.V. All rights reserved.

PACS: 42.55.Wd; 42.81.-i

Keywords: Nd-doped fiber; Fiber laser; W-type fiber

1. Introduction

Neodymium (Nd) ions have been well characterized in varieties of silica glass fibers and they provide competing radiative transitions in the near IR range, one around 1060 nm from the four-level

transitions, ${}^4F_{3/2} \rightarrow {}^4I_{11/2}$, and the other around 940 nm from the three-level ${}^4F_{3/2} \rightarrow {}^4I_{9/2}$. Especially the radiation near 920 nm has recently drawn intense attentions for applications in Raman fiber amplifier pumps for optical communications and high output blue laser by frequency doubling for optical displays [1–3]. In Nd-doped silica fibers, however, the 1060-nm transition dominates in the net optical gain due to its four-level natures [4–6]. The three-level system near 940 nm, ${}^4F_{3/2} \rightarrow {}^4I_{9/2}$, suffers from the ground state

* Corresponding author. Tel.: +82 62 970 2213/2245; fax: +82 62 970 2237.

E-mail addresses: swyoo@gist.ac.kr (S. Yoo), koh@gist.ac.kr (K. Oh).

absorption (GSA) and requires higher pumping power to support the population inversion. Therefore, a novel optical mechanism is required to selectively obtain the gain in the 940-nm region while suppressing the competing 1060-nm radiative transition. Recently, Nd-doped fiber laser at 938 nm with 11 W output has been reported using a large core fiber [7] which had a certain ratio of the fiber core to cladding for optimal operation. However, this report lacked the beam quality due to its multimode operation. Another technique was attempted by adopting a Nd-doped W-type fiber as an amplifier where 914-nm CW laser was reported [8] and S-band erbium-doped fiber amplifier was also adopted W-type fiber structure [9]. These prior works, however, have focused primarily on the experimental observations yet detailed analyses of waveguide designs for the laser cavity fiber and parametric comparisons between theories and experiments have been very rare until now.

Unlike conventional matched clad fibers, W-type fiber has the fundamental LP_{01} mode cut-off, λ_c , and the signal whose wavelength is longer than λ_c will leak out as a radiation mode to result in a short wavelength pass filter characteristic [10,11]. We will systematically apply this unique short-pass filter property of the W-fiber in a Nd-doped single mode silica fiber to effectively filter out the competing longer wavelength emission in 1060 nm ultimately facilitating 940 nm lasing. In this paper, we present detailed theoretical analyses on W-type fiber designs to obtain the optimal wavelength-selective transmission, high transparency in 940 nm and high attenuation in 1060 nm region. Parametric studies on the impact of fiber structural deviation over the location of the LP_{01} mode cut-off wavelength and bending loss are carried.

2. Fiber waveguide design

In Fig. 1, we present typical fluorescence spectra of Nd ions in silica glass fibers and the schematic for selective suppression of 1060 nm emission. The emission spectra of Nd ions do depend on glass hosts and as shown in Fig. 1(a), excited Nd

ions pumped by 808 nm laser generate two fluorescence bands one around 900–940 nm and the other 1090–1120 nm in $Ge_2O_3-SiO_2$ glass. On the while, the fluorescence of Nd ions in $Al_2O_3-SiO_2$ glass shifts to a shorter wavelength around 880–900 and 1060–1090 nm [12,13]. Taking account of the peaks around 900 and 1060 nm, suppression of emission above 1060 nm as well as high transparency below 940 nm is critical to prevent population inversion between ${}^4F_{3/2}$ and ${}^4I_{11/2}$ levels while preserving the transition of ${}^4F_{3/2} \rightarrow {}^4I_{9/2}$ to achieve laser acting in 900 nm region.

The proposed W-type fiber is illustrated in Fig. 1(b). The fiber is composed of three layers; Nd-doped core, depressed inner-cladding and silica cladding. Depressed index in the inner-cladding is achieved by doping fluorine or boron in silica, while the core index is raised by doping germanium and/or aluminum along with Nd ions. The main waveguide parameters are: (1) the refractive indices of the core, inner-cladding, and cladding denoted as n^+ , n^- and n_0 , respectively, (2) the core radius, a , and the inner-cladding radius, b . Refractive index differences between each layers are also denoted as $\Delta n^+ = (n^+ - n_0)$ and $\Delta n^- = -(n^- - n_0)$. These parameters define the LP_{01} mode cut-off wavelength.

Due to the short-pass filter characteristics, a Nd-doped W-fiber can be designed to induce a large attenuation near 1060 nm while keeping a high transparency in 940 nm region by locating the LP_{01} mode cut-off below 1060 nm. See the transmission curves in Fig. 1(b). For a given cut-off λ'_c in a fiber, we can furthermore fine-tune its location by bending the fiber in a certain radius of curvature. The bend will affect the effective index structure as shown in the bottom of Fig. 1(b) and will induce a larger attenuation in the longer wavelength to effectively shift λ'_c to a shorter wavelength. We, therefore, propose a novel technique to impose a highly selective attenuation in 1060 nm emission of Nd by designing a W-type waveguide with short-pass characteristics and wavelength-selective bend-induced loss therein.

The longitudinal components of the electric field in the LP_{01} mode in W-type fiber is given as below [11], and the coefficients, A_i , and subsequently the effective index of the mode can be com-

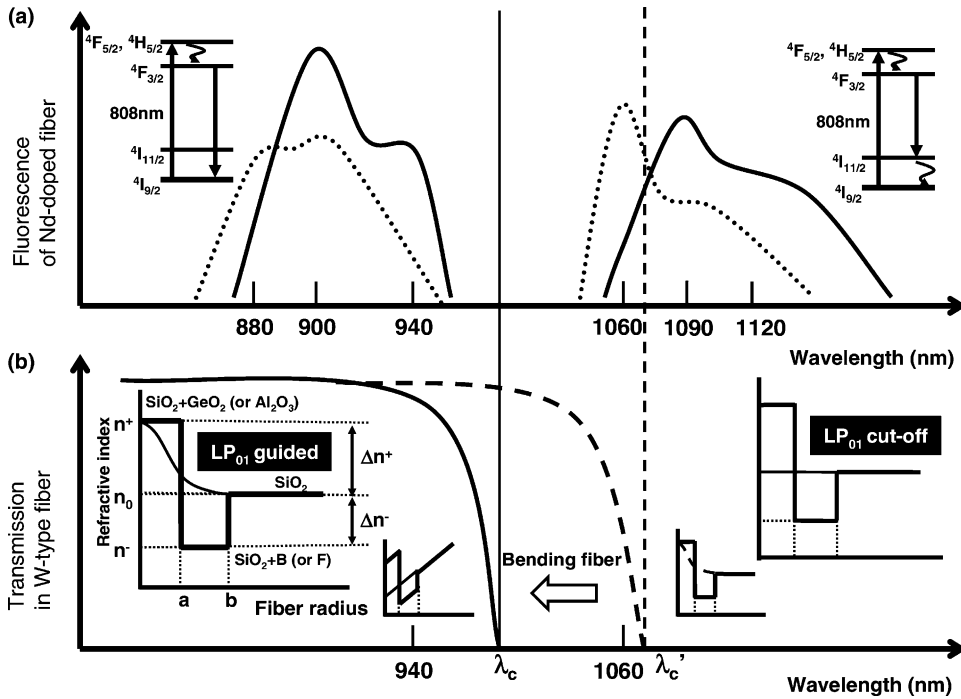


Fig. 1. (a) Fluorescence spectra and the energy level diagram Nd^{3+} ions in silica fibers and (b) structure of W-type fiber and schematics of suppression of 1060 nm. (a) The solid line and dotted line curves represent the fluorescence spectra of Nd ions from $\text{Ge}_2\text{O-SiO}_2$ and $\text{Al}_2\text{O}_3\text{-SiO}_2$ core fibers, respectively. It is noted that relative intensity near 940 nm increases in $\text{Ge}_2\text{O-SiO}_2$ fiber [12,13]. (b) Waveguide parameters of W-type fiber are shown in the inset figure on the left hand side along with the schematic of suppression of 1060 nm. Here n^+ , n^- , n_0 , a , and b are refractive index of core, depressed cladding, outer cladding, core radius, and depressed cladding radius, respectively. The refractive index differences are expressed as $\Delta n^+ = (n^+ - n_0)$ and $\Delta n^- = -(n^- - n_0)$. Firstly using the LP_{01} mode cut-off, the 1060 nm signal is leaked out as a radiation mode then the wavelength selective bending loss, which effectively shifts the cut-off from λ'_c to λ_c , is furthermore applied to suppress emission near 1060 nm.

puted by solving vectorial Maxwell’s equations at the boundaries

depressed by boron. The material dispersion of the doped layers was calculated using three term

$$E(r) = \begin{cases} A_0 J_0(u \frac{r}{a}) & \text{for } r < a \text{ in the core,} \\ A_1 I_0(w^- \frac{r}{b}) + A_2 K_0(w^- \frac{r}{b}) & \text{for } a < r < b \text{ in the inner - cladding,} \\ A_3 K_0(w \frac{r}{b}) & \text{for } r > b \text{ in the cladding,} \end{cases} \quad (1)$$

where J_0 , I_0 and K_0 are Bessel function of the first kind, modified Bessel functions of the first kind and the second kind, respectively. The normalized propagation constants, u , w^- and w , are defined as $u = a\{(k_0 n^+)^2 - \beta^2\}^{1/2}$, $w^- = b\{\beta^2 - (k_0 n^-)^2\}^{1/2}$ and $w = b\{\beta^2 - (k_0 n_0)^2\}^{1/2}$, respectively.

Here, we assumed the core index is raised by germanium and the inner-cladding index is

Sellmeier equations for binary germanosilica glass [14] and single Sellmeier oscillator expression for B-doped silica [15]. The wavelength is scanned until the effective index of the LP_{01} matches the refractive index of the silica cladding, at which the mode cut-off, λ_c , is evaluated. The routine is repeated for variation of fiber parameters to analyze their impacts on the location of λ_c . When we

varied one parameter in the analysis, all the rest of waveguide parameters were kept unchanged. In the calculation, the outer-cladding is assumed to expand infinitely.

Macro bending loss also affects the output spectrum of a fiber and is described as below in the LP₀₁ mode [16,17]

$$\alpha = \left(\frac{\pi v^8}{16aR_b w^3} \right)^{1/2} \exp \left(-\frac{4}{3} \frac{R_b}{a} \frac{w^3 \Delta}{v^2} \right) \times \left[\int_0^\infty \{1-f\} \frac{1}{a^2} F_0 r \, dr \right]^2 \bigg/ \int_0^\infty F_0^2 \frac{1}{a^2} r \, dr \quad (2)$$

with refractive index profile function, f ,

$$f = \begin{cases} 0, & 0 < r < a, \\ \frac{n^+ - n^-}{n^+ - n_0}, & a < r < b \\ 1 & r > b \end{cases} \quad (3)$$

and with refractive index parameter, Δ , is given by

$$\Delta = \frac{1}{2} \left(1 - \frac{n_0^2}{n^{+2}} \right) \quad (4)$$

where R_b is bending radius and F_0 is the electric field magnitude, which can be obtained from the solution of Eq. (1).

Note that the bending loss does depend on wavelength as in Eq. (2) inducing a higher loss at a longer wavelength, which will corroborate W-type fiber design to suppress 1060 nm emission while keeping the high transparency at 940 nm.

In order to analyze the effects of waveguide parameters and bending, we have designed W-type fibers by solving Eq. (1) to have the LP₀₁ cut-off wavelengths, λ_c , at an appropriate spectral position below 1060 nm. The parameters given in

Table 1 were determined by following procedure. Firstly, we set Δn^- as 0.003, which is a typical value achieved by B doping in SiO₂ glass layer in conventional fiber manufacturing process. In W-type fibers, the ratio of refractive index contrast between depressed inner-cladding and core, $\Delta n^-/\Delta n^+$, and the ratio of depressed cladding radius to core radius, b/a , are known to characterize the performance [10,11] and $\Delta n^-/\Delta n^+ = 1$ and $b/a = 2.5$ have shown a stable guiding performance against variations in the cut-off wavelength [10]. Therefore, the Δn^+ was decided to be 1.4600 to provide $\Delta n^-/\Delta n^+ = 1$. Then, the radii of core and depressed inner cladding were adjusted to satisfy both $b/a = 2.5$ and $\lambda_c < 1060$ nm. By the above considerations in waveguide design, λ_c was located at 1000 nm with 2.8 μm of core radius, a , and 7 μm of depressed cladding radius, b , for stable guiding performances at 940 nm and suppression of 1060 nm emission band.

3. Theoretical analysis

3.1. Impact of waveguide parameters

For the given W-fiber parameters in the first row of Table 1, the impacts of the core parameters such as n^+ , and a , over λ_c are analyzed and the results are summarized in Fig. 2. Considering conventional fiber fabrication techniques the variation ranges of the core parameters were chosen. In the region of $1.4535 < n^+ < 1.4605$ and $2.7 < a < 2.9$, the λ_c was plotted in Fig. 2(a) and (b), respectively. Note that the ranges correspond to $-0.034 < \Delta n^+/n^+ < 0.034\%$, and $-3.47 < \Delta a/a < 3.47\%$. With regard to these variations in core

Table 1

The parameters of calculated and fabricated Nd-doped W-type fibers for fiber lasers in 900 nm region (The parameters *in fabrication* were obtained by experimental measurements)

	Host glass of fiber core	n^+	n^-	n_0	a (μm)	b (μm)	r_f (μm)	λ_c in LP ₀₁ mode (nm)
In calculation	–	1.4600	1.4540	1.4570	2.80	7.00	–	1000
In fabrication	GeO ₂ -SiO ₂	1.4605	1.4540	1.4570	2.90	8.28	40	1120

n^+ , refractive index of core; n^- , refractive index of depressed inner cladding; and n_0 , refractive index of outer-cladding. a , core radius; b , depressed cladding radius from the center; and r_f , fiber radius. λ_c , cut-off wavelength evaluated from the parameters shown in the table.

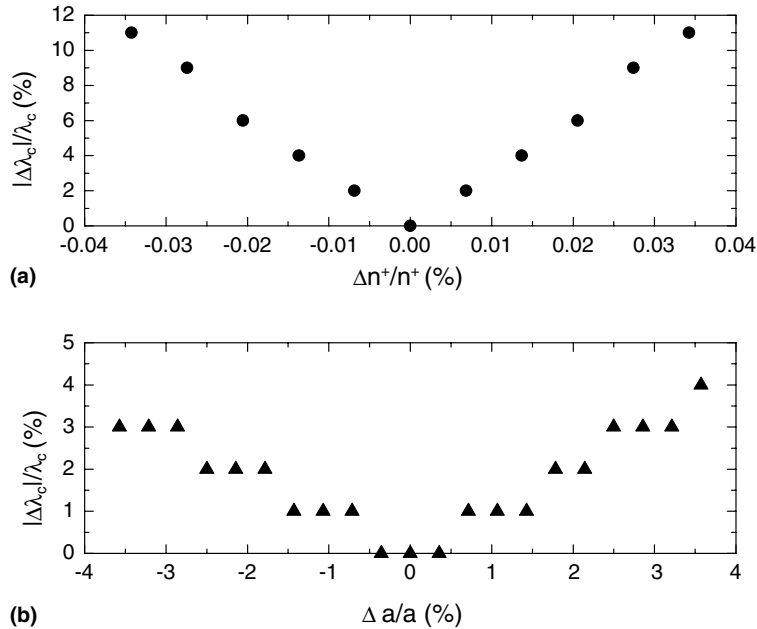


Fig. 2. Dependence of the LP₀₁ mode cut-off wavelengths, λ_c , on the variation of (a) refractive index of core, $\Delta n^+/n^+$ and (b) core radius, $\Delta a/a$. Here for the negative $\Delta n^+/n^+$ and $\Delta a/a$ decreases and its relative magnitude is plotted. The λ_c is 1000 nm when $\Delta n^+/n^+ = 0$ and $\Delta a/a = 0$. The initial fiber parameters are given in Table 1.

parameters, λ_c significantly shifts in a linear manner so that higher core index, positive $\Delta n^+/n^+$, and a larger core radius, positive $\Delta a/a$, shifted λ_c to a longer wavelength. It is found that λ_c , initially set at 1000 nm by the waveguide parameters in Table 1, increases to 1110 nm for 0.034% increment in $\Delta n^+/n^+$ and it decreases to 890 nm for 0.034% reduction. The curves were linearly fitted to find the slopes, $(|\Delta\lambda_c/\lambda_c|)/(\Delta n^+/n^+)$, to be 325.4. It is observed that λ_c is more sensitive to the variation in the core refractive index than core radius. Variation in $\Delta a/a$ within $\pm 3.47\%$ gave rise to change of λ_c from 970 to 1040 nm. The slope, $(|\Delta\lambda_c/\lambda_c|)/(\Delta a/a)$, was found to be -0.91 in the case of $\Delta a/a < 0$ and 1.09 for $\Delta a/a > 0$.

Similar to the core index, the ranges of inner-cladding index variation were chosen as $-0.034 < \Delta n^-/n^- < 0.034\%$ corresponding to ± 0.0005 variation of n^- . The shift of λ_c is plotted in Fig. 3(a). For the case of inner-cladding radius, b , it varied up to 14 μm (100%) from 5.6 μm (-20%) to investigate the behavior of λ_c for $\Delta b/b$ and the results are shown in Fig. 3(b). λ_c shifts to

longer wavelength with increasing $\Delta n^-/n^-$ as in Fig. 3(a) and shows a steeper increase in $\Delta n^-/n^- > 0$ than in $n^-/n^- < 0$. The linear fitting produced 20 and 30 nm shift in λ_c for -0.0005 and $+0.0005$ deviation of n^- , respectively. The cut-off wavelength, λ_c , monotonically decreases step-wise for increasing $\Delta b/b$ until $\Delta b/b$ reaches -5% from -20% of $\Delta b/b$. When the inner-cladding further expanded more, λ_c stays at 1000 nm. It is found that λ_c shows no shift in common fabrication error range in inner cladding radius, $\Delta b < \pm 0.1 \mu\text{m}$.

3.2. Wavelength selective macrobending loss and effective cut-off

It is noteworthy to find the practical implications of shift range of λ_c for the fiber parameter variations. For the core radius variation of 3.47%, or equivalently 0.1 μm deviation, λ_c was found to shift up to 1040 nm. This spectral location might not be far enough from the 1060 nm emission band for it to be suppressed. Consequently, Nd-doped W-fibers should require precise

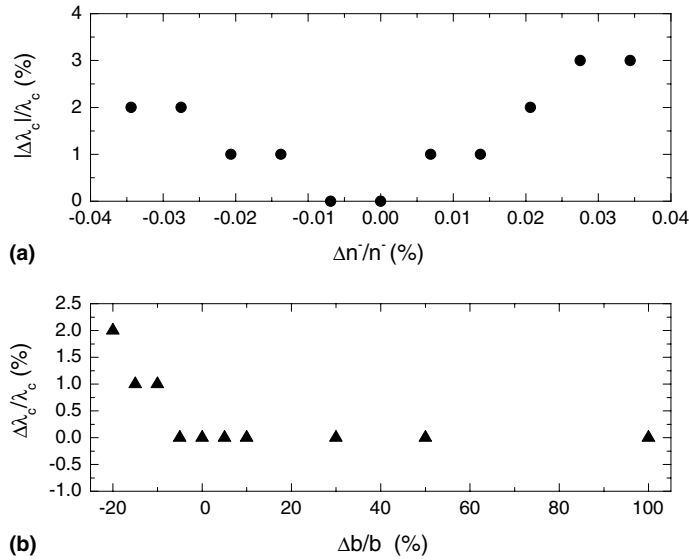


Fig. 3. Dependence of cut-off wavelengths, λ_c , on the variation of (a) refractive index of depressed cladding, $\Delta n^-/n^-$, and (b) depressed cladding radius, $\Delta b/b$. (b) Here for the negative $\Delta n^-/n^-$ λ_c decreases and its relative magnitude is plotted. The λ_c is 1000 nm when $\Delta n^-/n^-$ and $\Delta b/b = 0$. The initial fiber parameters are given in Table 1.

radius control within $\pm 0.1 \mu\text{m}$. For the core index variation over 0.02%, or equivalently 0.0005 in refractive index, λ_c exceed 1060 nm, which will allow the guidance of 1060 nm emission. These ranges of variations could be achieved only by elaborated control even using the state of art fabrication facility. In order to circumvent these demanding fabrication accuracies, we propose that the wavelength dependent macro-bending loss be induced on a W-type fiber to further fine-tune the spectral position of λ_c . In this proposed technique, a W-type fiber with a longer cut-off, λ'_c as is shown in Fig. 1(b), is fabricated with a less demanding fabrication tolerance. Then the fiber is wound with a certain radius of curvature to induce bending loss that grows exponentially with increasing wavelength [18], which will effectively shift the cut-off to the appropriate λ_c .

Bending losses at 940 and 1060 nm were calculated for the proposed W-fiber using Eq. (2) to analyze the wavelength selectivity, and the results are plotted in Fig. 4 as a function of $\Delta n^+/n^+$. Since only the variation in n^+ resulted in λ_c shift beyond 1060 nm in the previous parametric studies, we will confine our discussion on the core index variation.

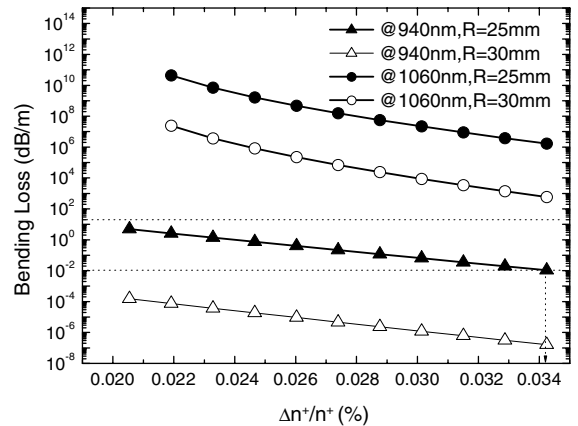


Fig. 4. Bending loss of W-type Nd-doped fiber as a function of refractive index of core, $\Delta n^+/n^+$. Under the lower horizontal line at 10^{-2} dB/m, the transparency in 900 nm region is maintained while the wavelengths in 1060 nm region is suppressed above the upper horizontal line at 20 dB/m with 10m long W-type fibers.

In Fig. 4, when the allowed $\Delta n^+/n^+$ is 0.034%, the bending losses at 940 and 1060 nm with $R = 25$ mm are 10^{-2} and 2×10^6 dB/m, respectively. Assuming that the fiber length of 10 m is wound on a post of $R = 25$ mm, the emission beyond

1060 nm will be effectively suppressed by bending loss over 2×10^7 dB while keeping a high transparency of 0.1 dB at 940 nm. Bending losses with $R = 30$ mm shows similar results such as 2×10^{-6} dB at 940 nm and 6×10^3 dB at 1060 nm with 10m long Nd-doped W-fiber. Therefore, the cut-off shift induced by the fabrication inaccuracy of 0.0005 in refractive index of the core, $\Delta n^+/n = 0.034\%$, can be compensated by bending loss. Note that the fiber length of 10 m is arbitrary but it is representing actual fiber length in rare earth doped fiber lasers. Two horizontal dotted lines are added on Fig. 4, which correspond to the bending losses of 10^{-2} and 20 dB/m. These will serve as a guideline for 10^{-1} dB loss in 900 nm region and 200 dB loss for 1060 nm band for 10 m long fibers [9].

In order to further analyze the effect of bending loss in the spectral domain, we calculated the bending loss as a function of wavelength for various bending radii as in Fig. 5. Here, we examined specific case of $\Delta n^+/n = 0.034\%$ with the cut-off wavelength at 1110 nm. By applying bending to this W-fiber of 10 m long, wavelength dependent loss will result in effective shift of λ_c toward the shorter wavelength as schematically illustrated in

Fig. 1(b). The cut-off wavelength has been determined at the point where the maximum transmitted power drops by 2 dB [19]. Assuming 10 long fiber, we drew 0.2 dB/m horizontal line in Fig. 5(a) to estimate the effective cut-offs for different bending radii. In Fig. 5(a), the effective λ_c moves to 1060, 1015 and 958 nm for $R = 35, 30,$ and 25 mm, respectively. However, the cut-off shift alone is not enough to suppress the competing emission at the longer wavelength and we need to confirm more than 200 dB loss as recommended in [9]. In Fig. 5(b), losses over 200 dB can be achieved in 10 m long W-fibers above 1077, 1040 and 990 nm for $R = 35, 30$ and 25 mm, respectively. See the intersection of the plot with the horizontal line at 20 dB/m. These results clearly show that the bending loss provides an effective post-fiber fabrication technique to control the LP_{01} mode cut-off wavelength of W-fiber, compensating fiber parameter deviations.

4. Experimental results and discussion

Nd-doped W-type fiber preform was fabricated by conventional modified chemical vapor

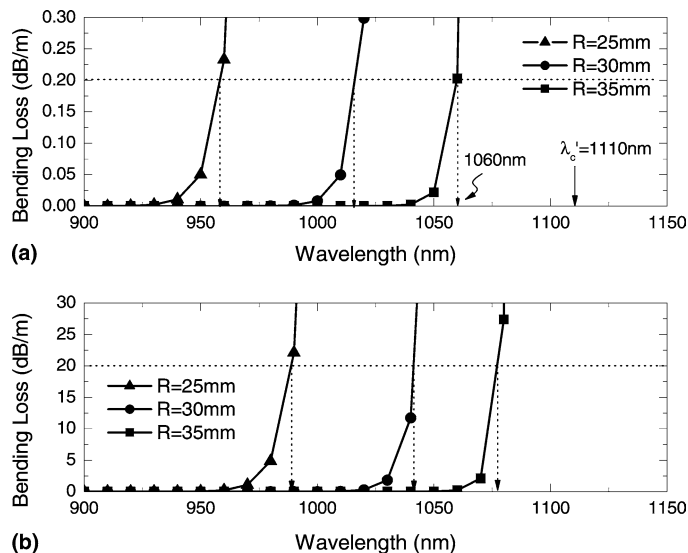


Fig. 5. Bending loss vs. wavelength in Nd-doped W-fiber. λ_c is deviated cut-off wavelength induced by 0.0005 variation in n^+ . The horizontal lines in (a) and (b) indicate the effective cut-off condition and the complete suppression in 1060 nm region with 10m fiber length, respectively.

deposition (MCVD) process along with solution doping techniques [20]. The composition of $\text{GeO}_2\text{-SiO}_2$ was chosen as core material to take advantage of higher emission cross-section in 900 nm region compared to $\text{Al}_2\text{O}_3\text{-SiO}_2$ [12,13]. The concentration of Nd was 240 ppm distributed over the whole core. The preform was prepared in D-shape to enhance the overlap between Nd ions in the core and pump guided along the cladding. Then the fibers were drawn with 80 μm diameter. The detailed parameters of fabricated Nd-doped W-fiber are given in the second row of Table 1. The fiber has its LP_{01} mode cut-off at 1120 nm due to fabrication error. However, the variations in core radius, a , and core refractive index, n^+ , were kept within the range discussed in the theoretical analyses.

The fiber laser setup is presented in Fig. 6. A Fabry–Perot oscillator was formed by two dichroic mirrors at the end of fiber along with focusing optics. The laser performance was investigated with bi-directional pumping at 808 nm with the maximum coupled power of 4.5 and 3.5 W at each end. The fiber was wound in an appropriate bending radius to further suppress 1060 nm emission. One end of the fiber was angle-cleaved to prevent fresnel reflection and the output laser wavelength in 900 nm region was tuned by a bulk grating at the angle-cleaved end of the fiber cavity.

In Fig. 7, we show the effect of bending in λ_c shift in experiment. The straight fiber of 1.5 m showed the LP_{01} mode cut-off beyond 1060 nm, the solid line. By bending the fiber, however, the effective the effective cut-off shifts to a shorter wavelength to result in high transparency below 940 nm and large attenuation beyond 1060 nm. The effective λ_c shifted to a shorter wavelength with reducing bending radius as predicted in theo-

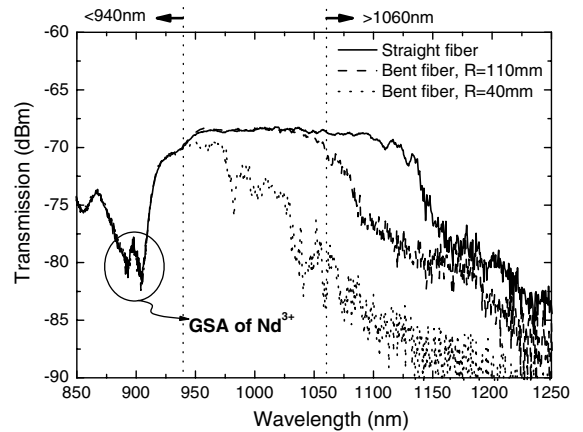


Fig. 7. Suppression of guidance above 1060 nm by bending. Note that the absorption around 900 nm is the Ground State Absorption (GSA) of Nd ions.

retical analysis. The results clearly manifest that the laser acting in 900 nm region is obtainable by our proposed scheme. The absorption peak around 900 nm is caused by ground state absorption (GSA) subject to $^4\text{I}_{9/2} \rightarrow ^4\text{F}_{3/2}$ of Nd^{3+} .

The typical spectrum of fiber laser operating in 900 nm region is shown in solid line in Fig. 8 along with measured emission cross-section in dotted line. Here, we bent the fiber in the radius of 30 mm. The emission cross-section was obtained from the side-measured fluorescence spectra of a straight fiber using the relation by [6,21,22],

$$\sigma_c = \frac{\lambda^4 I_c(\lambda)}{8\pi c n^2 \tau \int I_c(\lambda) d\lambda} \quad (5)$$

where I_c is fluorescence intensity in $[\text{W}/\text{m}^2]$, τ is life time, $\sim 490 \mu\text{s}$ in our experiments, n is refractive index of doped glass, and c is the velocity of light.

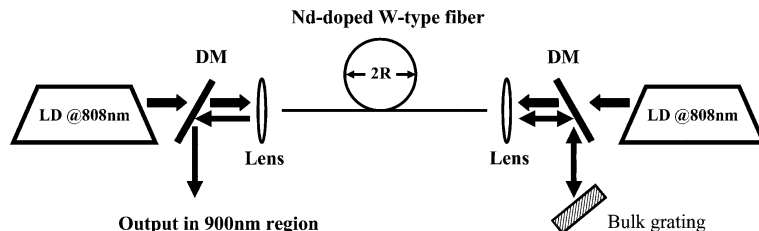


Fig. 6. Fiber laser setup. DM: Dichroic mirror, LD: Laser diode, and R: Bending radius.

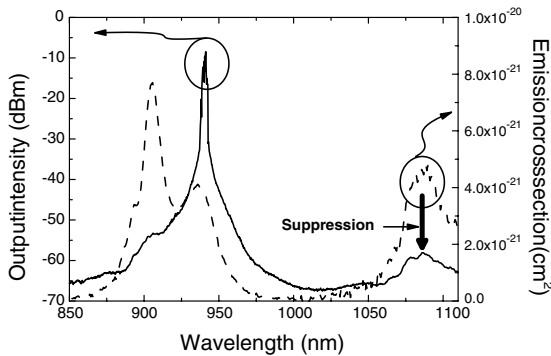


Fig. 8. Typical laser spectrum operating in 900 nm region in solid line and measured emission cross-section in dotted line.

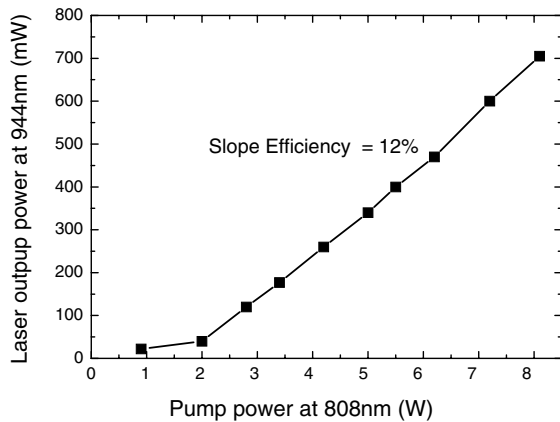


Fig. 9. Slope efficiency of Nd-doped W-type fibers with respect to launched pump power.

In Fig. 8, we experimentally demonstrated that our proposed highly wavelength selective loss mechanism-W-type fiber along with macro-bending loss, can effectively manipulate the net emission cross-section of Nd ions to suppress lasing in 1060 nm region obtaining CW laser action at 944 nm.

In Fig. 9, we obtained the slope efficiency of 12% with respect to the launched pump power at 944 nm with 57 m fiber length. The threshold was around 2 W. The wavelength-tunability was investigated and the fiber showed laser operating in 932–953 nm with highest peak power of 705 mW at 944 nm for the available pumps. The output beam was found to be in the single mode with $M^2 = 1.14$ [23].

5. Conclusions

Continuous wave oscillation at 944 nm was successfully demonstrated from Nd-doped fiber by implementing a novel highly wavelength selective loss mechanism-the LP_{01} mode cut-off in W-type fiber along with macro-bending loss. The wavelength selectivity of the proposed structure has been theoretically analyzed for variations in fiber waveguide parameters. The shift in LP_{01} cut-off wavelength significantly depends on the core parameters, especially the core refractive index, rather than inner-cladding parameters. Macro-bending loss was found to be a useful post-fiber technique to control the effective cut-off wavelength. The theoretical analyses have been successfully confirmed by experiments in a fiber Fabry–Perot cavity with Nd-doped W-type fiber along with macro-bending to achieve CW oscillation at 944 nm suppressing 1060 nm emission.

Acknowledgment

This work was supported by the Brain Korea-21 Information Technology Project, Ministry of Education, Korea.

References

- [1] H. Fuchs, M.A. Tremont, O. Casel, R. Wallenstein, in: Proceedings of the Lasers and Electro-Optics Society, vol. 2, 2002, p. 442.
- [2] G.S. Maciel, A. Biswas, R. Kapoor, P.N. Prasad, Appl. Phys. Lett. 76 (15) (2000) 1978.
- [3] V. Gaebler, B. Liu, H.J. Eichler, Z. Zhang, D. Shen, Opt. Lett. 25 (18) (2000) 1343.
- [4] L. Reekie, I.M. Jauncey, S.B. Poole, D.N. Payne, Electron. Lett. 23 (17) (1987) 884.
- [5] I.P. Alcock, A.I. Ferguson, D.C. Hanna, A.C. Tropper, Opt. Lett. 11 (11) (1986) 709.
- [6] M.J.F. Digonnet, E. Snitzer, in: M.J.F. Digonnet (Ed.), Rare Earth Doped Fiber Lasers and Amplifiers, Marcel Dekker, NY, 1993.
- [7] J.W. Dawson, R. Beach, A. Drobshoff, Z. Liao, D.M. Pennington, S.A. Payne, L. Taylor, W. Hackenberg, D. Bonaccini, in: Proceedings of the Advanced Solid-State Photonics, Santa Fe, NM, USA, 2004, MD8.
- [8] T.J. Kane, G. Keaton, M.A. Arbore, D.R. Balsley, J.F. Black, J.L. Brooks, M. Byer, L.A. Eyres, M. Leonardo, J.J.

- Morehead, C. Rich, D.J. Richard, L.A. Smoliar, Y. Zhou, in: *Proceedings of the Advanced Solid-State Photonics*, Santa Fe, NM, USA, 2004, MD8.
- [9] M. Arbore, Y. Zhou, H. Thiele, J. Bromage, L. Nelson, in: *OFC 2003 WK2*, 2003, p. 374.
- [10] L.G. Cohen, D. Marcuse, W.L. Mammel, *Trans. Microwave Theory Tech.* MTT 30 (10) (1982) 1455.
- [11] M. Monerie, *J. Quantum Electron.* QE-18 (4) (1982) 535.
- [12] P.D. Dragic, G.C. Papen, *Photon. Technol. Lett.* 11 (12) (1999) 1593.
- [13] K. Arai, H. Namikawa, K. Kumata, T. Honda, Y. Ishii, T. Handa, *J. Appl. Phys.* 59 (10) (1986) 3430.
- [14] J.W. Fleming, *Appl. Opt.* 23 (1984) 4486.
- [15] S.H. Wemple, D.A. Pinnow, T.C. Rich, R.E. Jaeger, L.G. Van Uitert, *J. Appl. Phys.* 44 (12) (1973) 5432.
- [16] A.W. Snyder, J.D. Love, *Optical Waveguide Theory*, Chapman & Hall, NY, 1983.
- [17] S.J. Garth, *J. Lightwave Technol.* 7 (1989) 1889.
- [18] D. Marcuse, *J. Quant. Electron.* 29 (1993) 2957.
- [19] F.C. Allard, *Fiber Optics Handbook for Engineers and Scientists*, McGraw-Hill, NY, 1990, Chapter 4.
- [20] J.E. Townsend, S.B. Poole, D.N. Payne, *Electron. Lett.* 23 (7) (1987) 329.
- [21] R.R. Jacobs, M.J. Weber, *J. Quantum Electron.* QE-12 (2) (1976) 102.
- [22] W.F. Krupek, *J. Quantum Electron.* QE-10 (4) (1974) 450.
- [23] D.B.S. Soh, S. Yoo, J.K. Sahu, L.J. Cooper, S. Baek, K. Oh, in: *Proceedings of the Advanced Solid-State Photonics*, Santa Fe, NM, USA, 2004, MD9.